Materials Characterization 97 (2014) 11–17

Contents lists available at ScienceDirect

Materials Characterization

journal homepage: www.elsevier.com/locate/matchar

Abnormal grain growth in AISI 304L stainless steel

M. Shirdel [a], H. Mirzadeh [a,c,*], M.H. Parsa [a,b,c]

[a] School of Metallurgy and Materials Engineering, College of Engineering, University of Tehran, P.O. Box 11155-4563, Tehran, Iran
[b] Center of Excellence for High Performance Materials, School of Metallurgy and Materials Engineering, University of Tehran, Tehran, Iran
[c] Advanced Metalforming and Thermomechanical Processing Laboratory, School of Metallurgy and Materials Engineering, University of Tehran, Tehran, Iran

ARTICLE INFO

Article history:
Received 8 April 2014
Received in revised form 30 July 2014
Accepted 27 August 2014
Available online 28 August 2014

Keywords:
Austenitic stainless steel
Grain growth
Secondary recrystallization

ABSTRACT

The microstructural evolution during abnormal grain growth (secondary recrystallization) in 304L stainless steel was studied in a wide range of annealing temperatures and times. At relatively low temperatures, the grain growth mode was identified as normal. However, at homologous temperatures between 0.65 (850 °C) and 0.7 (900 °C), the observed transition in grain growth mode from normal to abnormal, which was also evident from the bimodality in grain size distribution histograms, was detected to be caused by the dissolution/coarsening of carbides. The microstructural features such as dispersed carbides were characterized by optical metallography, X-ray diffraction, scanning electron microscopy, energy dispersive X-ray analysis, and microhardness. Continued annealing to a long time led to the completion of secondary recrystallization and the subsequent reappearance of normal growth mode. Another instance of abnormal grain growth was observed at homologous temperatures higher than 0.8, which may be attributed to the grain boundary faceting/defaceting phenomenon. It was also found that when the size of abnormal grains reached a critical value, their size will not change too much and the grain growth behavior becomes practically stagnant.

1. Introduction

Abnormal grain growth or secondary recrystallization is characterized by a bimodal grain size distribution as a result of the rapid growth of a small number of large grains [1,2]. It is frequently observed that secondary recrystallization occurs when normal grain growth is restrained. Therefore, the main factors which lead to abnormal grain growth are texture, second-phase particles, surface effects and grain boundary faceting/defaceting [1–5].

By contrast, the normal grain growth is defined as a uniform increase in the average grain size of a polycrystalline aggregate by grain boundary migration as a result of annihilation of smaller grains. During this process, the distribution of grain size remains relatively uniform and a monomodal grain size distribution will be resulted [6–10]. It is also worth mentioning that the 3D grain growth has been recently discussed by MacPherson and Srolovitz [3].

There are several criteria to distinguish between AGG and NGG. A useful criterion states that abnormal grain growth is commenced when the ratio of the size of the maximum observed grain to the average grain size becomes greater than 5 [11]. Rios [12] has established a useful criterion, which considers that when the relative size of the candidate grain for abnormal growth (D_{Abnorm}) increases, i.e. $d(D_{Abnorm}/D_{average})/dt > 0$, abnormal grain growth occurs. D_{max} and $D_{average}$ are the sizes of the maximum observed grain and the average grain size, respectively.

The aims of this study is to investigate the microstructural evolution during abnormal grain growth in an AISI 304L austenitic stainless steel and elucidating the metallurgical phenomena behind it.

2. Experimental Materials and Procedures

Commercial type 304L stainless steel with chemical composition of 0.023 wt.% C–18.47 wt.% Cr–8.05 wt.% Ni–0.476 wt.% Si–1.43 wt.% Mn–0.09 wt.% Mo–0.003 wt.% Ti–0.129 wt.% V–0.128 wt.% Nb was used in this study. The microalloy additions in austenitic stainless steels have been found to inhibit grain growth due to finely dispersed carbides or carbonitrides [13].

The samples were annealed at temperatures between 700 °C and 1200 °C and then immediately quenched in water. Afterwards, the specimens were pickled in a solution containing 15% HNO_3 (65% strength), 5% HF (50% strength) and 80% water to dissolve the oxide layer formed at the surface [14], which reduces the requirement of severe mechanical grinding. Therefore, the strain-induced martensitic transformation [15] at the surface layer will be largely avoided. Due to the metastability nature of austenite in austenitic stainless steels, severe mechanical grinding might produce some strain-induced martensite on the surface [16,17], especially in coarse austenite grains. A typical example is shown in Fig. 1.

Electrolytic etchings in a 60% HNO_3 solution at 2 V [18] and in a solution containing 1 g CrO_3 solved in 100 ml water at 8 V [19]

* Corresponding author at: School of Metallurgy and Materials Engineering, College of Engineering, University of Tehran, P.O. Box 11155-4563, Tehran, Iran.
E-mail addresses: mshirdel1989@ut.ac.ir (M. Shirdel), hmirzadeh@ut.ac.ir (H. Mirzadeh), mhparsa@ut.ac.ir (M.H. Parsa).

http://dx.doi.org/10.1016/j.matchar.2014.08.022
1044-5803/

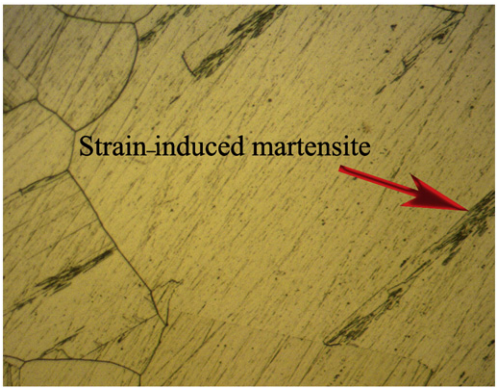

Fig. 1. Optical micrograph of the sample annealed at 1150 °C for 4 h.

were used to reveal austenite grain boundaries and the dispersed carbides, respectively.

3. Results and Discussions

3.1. The Effect of Annealing Temperature

Optical micrographs of AISI 304L stainless steel after 3 h annealing at different temperatures are shown in Fig. 2. As can be seen in this figure, substantial grain growth happens by annealing at elevated temperatures. A polycrystalline material contains a large number of grain boundaries, which represent high-energy areas because of the inefficient packing of the atoms. A lower overall energy is obtained in the material if the amount of grain boundary area is reduced by grain growth.

Fig. 2 also shows that, in some annealing conditions, abnormal grain growth occurs. Due to some reasons such as sluggish diffusion in austenite, low mobility of high angle grain boundaries, particles and low driving force [2], there is no considerable grain growth at homologous temperatures lower than 0.65 (<850 °C). At homologous temperatures between 0.65 and 0.7 (900 °C), a transition in grain growth mode from normal to abnormal can be observed. The growth mode for the investigated annealing times (1 to 4 h) was detected as normal after annealing at homologous temperatures higher than 0.7 but lower than 0.8 (1100 °C), which can be seen in Fig. 2 for annealing temperatures of 1000 °C and 1050 °C. To further verify these findings, analysis was performed for annealing temperature of 950 °C as shown in Fig. 3, which is consistent with the mentioned trend. Finally, the mode of grain growth reverted to abnormal by annealing at homologous temperatures equal to and higher than 0.8.

3.2. Secondary Recrystallization

Fig. 4 shows the microstructural evolution during annealing at 850 °C. It can be seen that the grain growth mode is normal after annealing for 1 h and 2 h. However, a transition in grain growth mode from normal to abnormal can be observed after annealing for 3 h. This situation continues for a soaking time of 4 h. The question of what will happen if annealing is continued at much higher annealing times arises. However, the growth kinetics is slow at such a temperature. To overcome

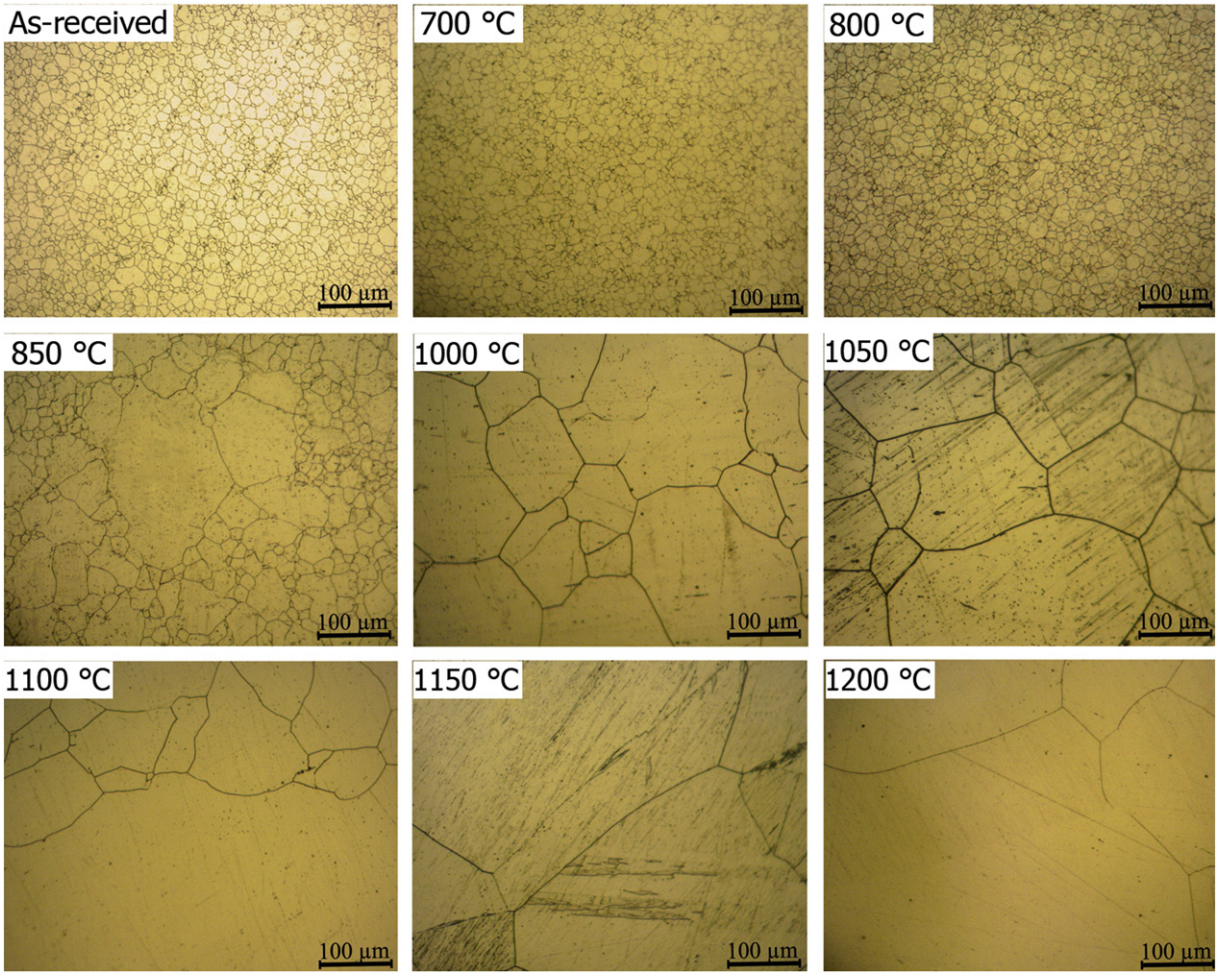

Fig. 2. Optical micrographs of AISI 304L stainless steel after annealing for 3 h at different temperatures.

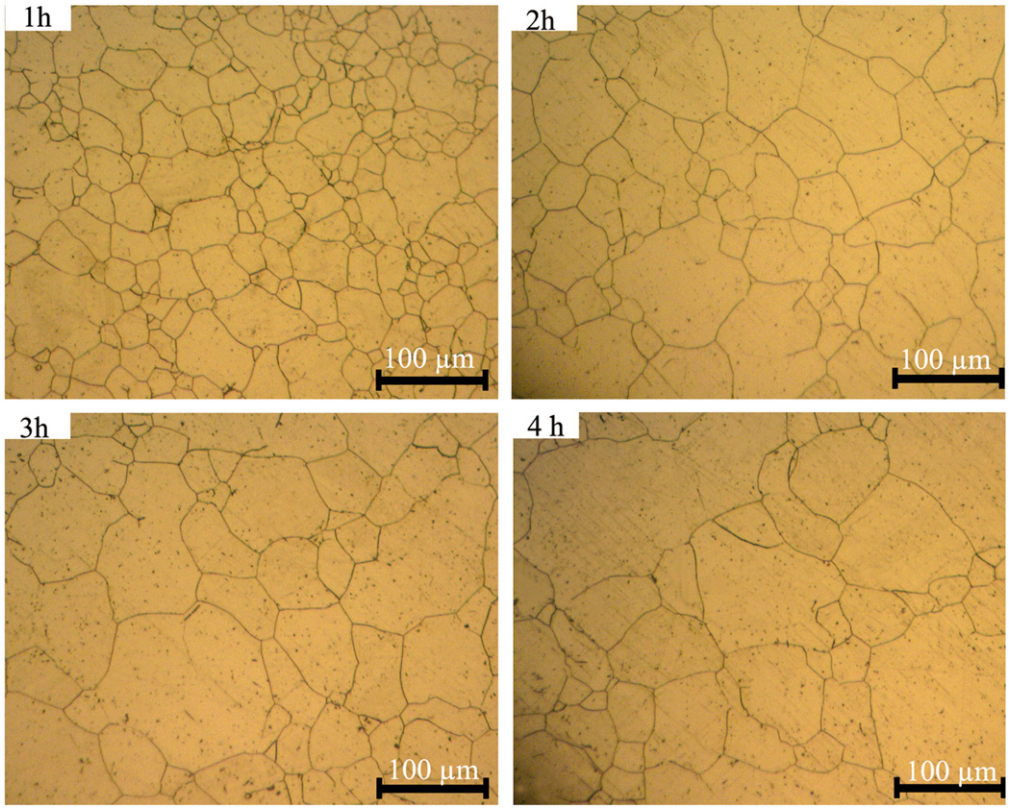

Fig. 3. Optical micrographs of AISI 304L stainless steel after annealing at 950 °C.

this difficulty, a microstructural evolution at a higher temperature (900 °C) for a wide range of soaking times was studied.

Fig. 5 shows the microstructural evolution during annealing at 900 °C with corresponding grain size distribution histograms. In the first 15 min at a temperature of 900 °C, no considerable coarsening happened and the grain growth mode is normal as can be seen in Fig. 5. However, by further annealing till 30 min, a transition from normal to abnormal mode has been obtained, which resulted in a bimodal

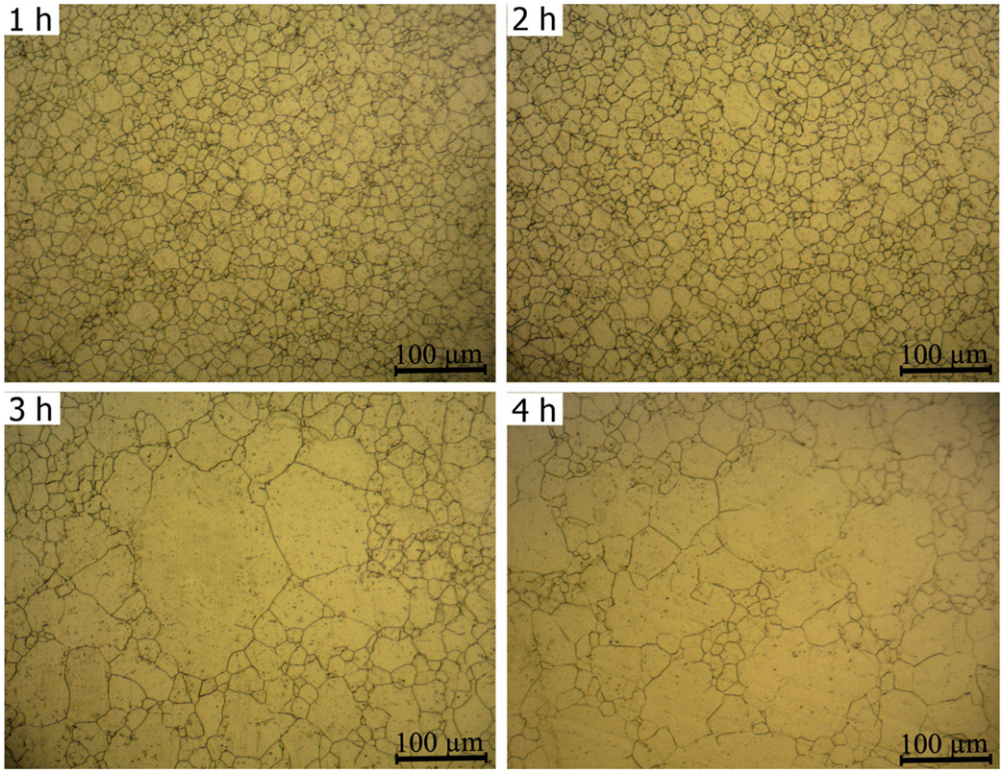

Fig. 4. The microstructural evolution of AISI 304L stainless steel during annealing at 850 °C.

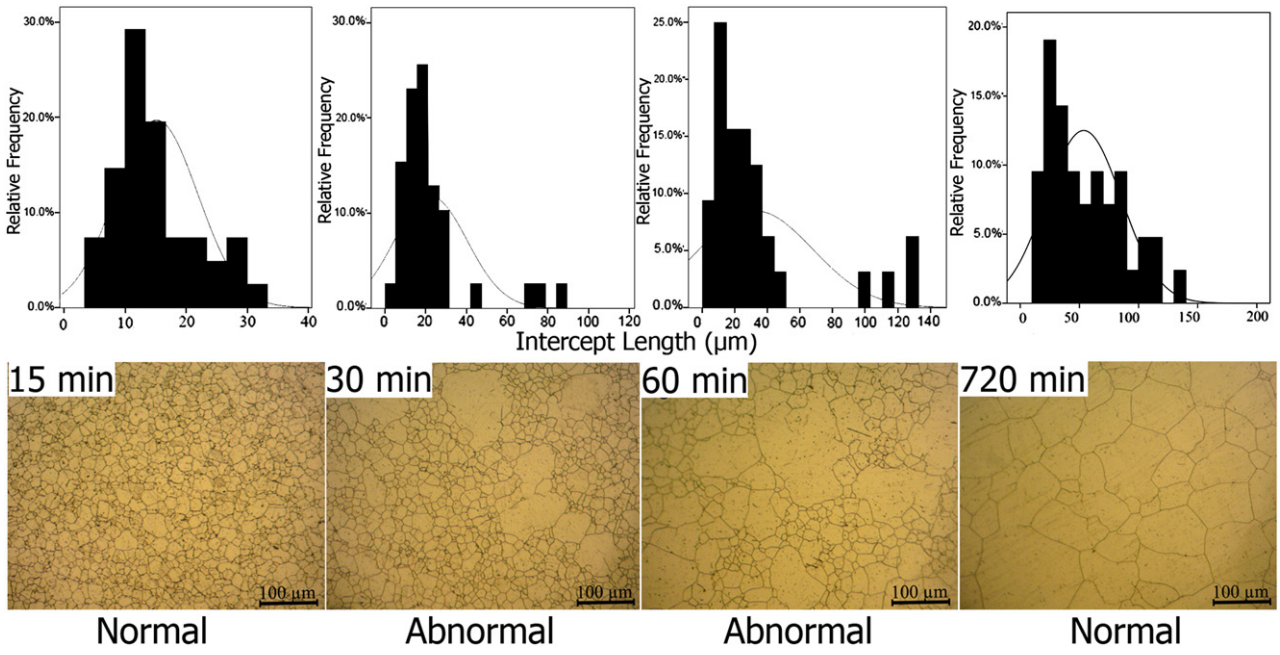

Fig. 5. Optical micrographs and the corresponding grain-size distribution histograms obtained upon annealing at 900 °C.

distribution of grain size. By continued annealing for 60 min, the bimodality of the histogram becomes more evident. These observations can be ascribed to dissolution/coarsening of carbides and the resultant selective growth of a few large grains. Finally, Fig. 5 shows that by long time annealing (12 h), the grain growth mode will revert to normal. This can be attributed to the completion of secondary recrystallization [20].

As discussed before, the investigated 304L stainless steel in the current study contains several carbonitride forming elements such as Ti, V and Nb. The optical micrograph in Fig. 6 shows that some carbide particles are present after annealing at 900 °C for 1 h. This is consistent with the corresponding X-ray diffraction pattern shown in Fig. 6 (using a Philips PW-3710 diffractometer with Cu Kα radiation), which shows a new diffraction peak pertaining to a complex carbide (composed of Ti, Cr, Fe, and C).

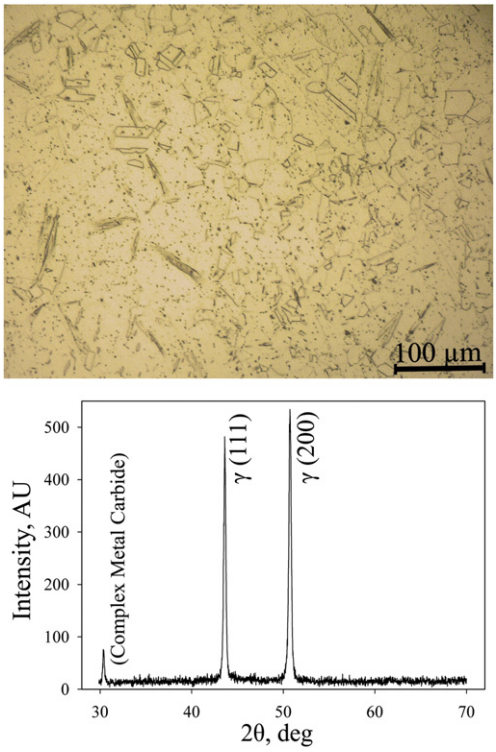

Fig. 6. Optical micrographs and the corresponding XRD after annealing at 900 °C for 1 h.

To distinguish the carbide particles among the darkly etched spots of the optical micrograph of Fig. 6, observations were carried out in a Vega Tescan scanning electron microscope (SEM) equipped with an energy dispersive X-ray analyzer (EDAX) and the results are shown in Fig. 7. Fig. 7a shows the typical morphology of the carbides in the studied alloy at a high magnification and the corresponding EDAX spectra in Fig. 7b show that the carbide particles are rich in Ti and also have other elements such as V, Cr, and Fe. This is consistent with the XRD results shown in Fig. 6. The EDAX spectra of Fig. 7c show that the elements such as Fe, Mn, Cr, Ni, V, Si, and C are present in the austenite matrix. Therefore, titanium only exists as carbides in the investigated alloy. Finally, as shown in Fig. 7d, the elements present in the pitted regions are practically similar to those of the matrix (Fig. 7c). Moreover, Vickers microhardness tests with an indentation force of 5 kg were performed on a carbide particle and on the matrix as shown in Fig. 7b and c. The size of the indentation in Fig. 7b is significantly smaller than that of Fig. 7c, which signifies the presence of carbides. It is clear that the smaller the indentation, the harder the material.

At first 15 min of annealing at 900 °C, the small and widely dispersed carbide particles seem to be effective in the inhibition of grain growth. Further annealing to 30 min, results in partial dissolution/coarsening of carbides, which leads to abnormal grain growth in the depleted zones. This situation becomes severe by continued annealing to 1 h. Finally, by long time annealing (12 h), the grain growth mode reverts to normal due to the completion of secondary recrystallization. This is also the case for annealing at 850 °C for much longer soaking times. These findings can be better visualized by plotting the ratio of the maximum observed grain size to the average grain size as a function of annealing time as shown in Fig. 8. At first 15 min of annealing and for 12 h annealing, the ratio of the maximum observed grain size to the average grain size is relatively low. It is interesting to note that annealing for 30 min is the most severe case of abnormality based on the results shown in Fig. 8.

At very high annealing temperatures (above 0.8 T_m), abnormal grain growth behavior was observed again. An extreme case is shown in Fig. 2

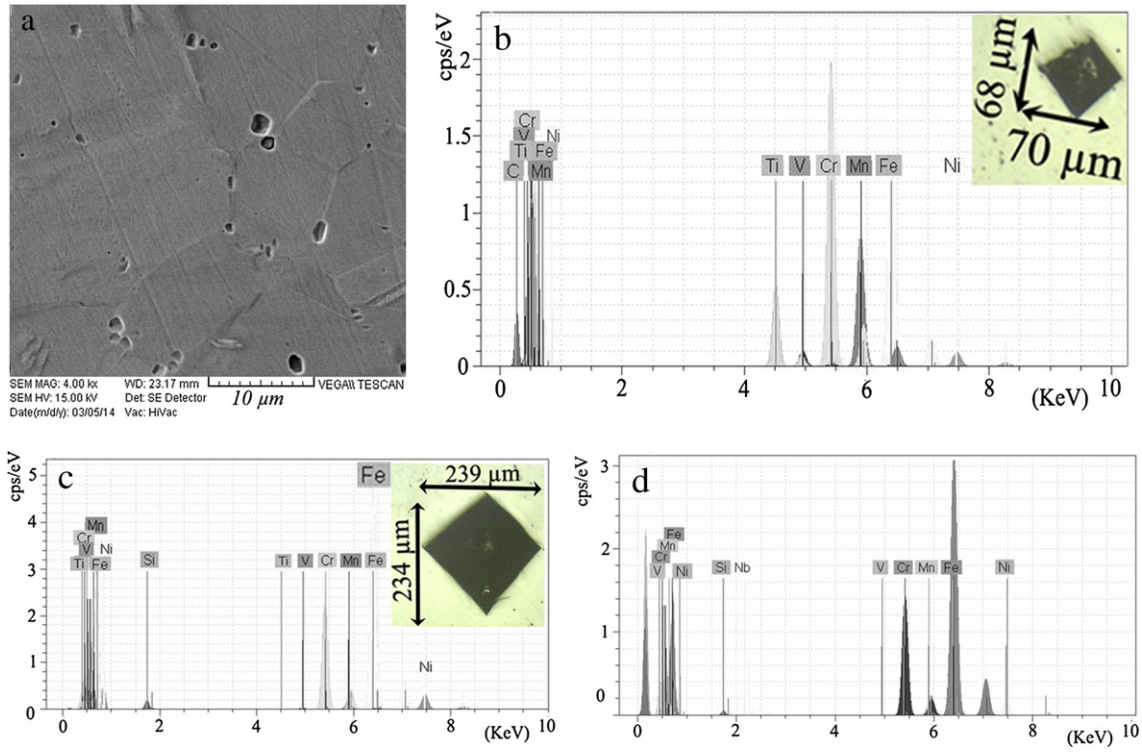

Fig. 7. The analyses performed on the sample annealed at 900 °C for 1 h: (a) SEM image, (b) EDAX spectra of a typical carbide particle and the corresponding microhardness indentation, (c) EDAX spectra of the matrix and the corresponding microhardness indentation, and (d) EDAX spectra of a region detected as a pit.

for a specimen annealed at 1100 °C for 3 h. The probability of AGG due to the coarsening or dissolution of precipitates at such very high temperature is negligible in the present work. Therefore, the abnormality in grain growth at these high temperatures may be attributed to grain boundary faceting/defaceting phenomenon as demonstrated for 316L stainless steel and other metals [4,5].

3.3. The Stagnancy of the Grain Growth Behavior

Careful inspection of histograms in Fig. 5 makes this point clear that by annealing beyond a critical time (probably 1 h at 900 °C), the growth rate of the abnormally grown grains significantly drops (Fig. 9). This is due to this fact that the number of consumable small matrix grains available for abnormal growth decreases. It means that when the size of the abnormal grains reached a critical value, their size will not change too much and the grain growth behavior becomes practically stagnant. For example, the ratio of the largest detected grain after 12 h annealing at 900 °C to the largest observed grain in 1 h annealing at 900 °C is about 1.1 as shown in Fig. 9.

3.4. Some Observed Microstructural Features During Abnormal Grain Growth

The following phenomena during grain growth, especially abnormal grain growth, were observed or supposed to be occurred for the investigated material: sub-boundary enhanced solid-state wetting (Fig. 10a), shrinkage/annihilation of grains with less than 6 sides (Fig. 10b), movement of concave grain boundaries toward their centers of curvature (Fig. 10b), and probably grain boundary faceting (Fig. 10c and d).

As argued by Ko et al. [21], precipitates inhibit not only grain boundary migration but also solid-state wetting along a triple junction if they

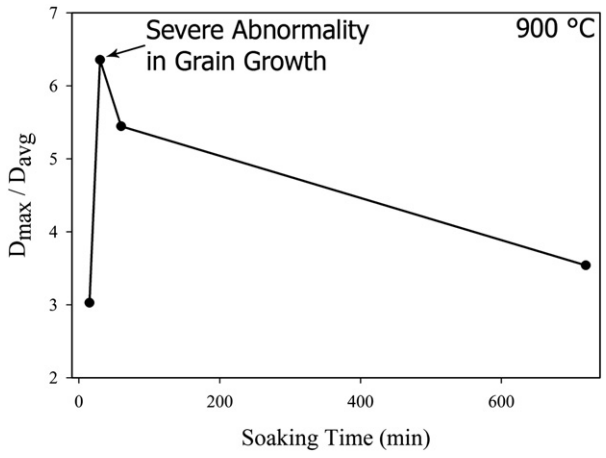

Fig. 8. The plot showing the ratio of the size of the maximum observed grain to the average grain size vs. soaking time for the sample annealed at 900 °C.

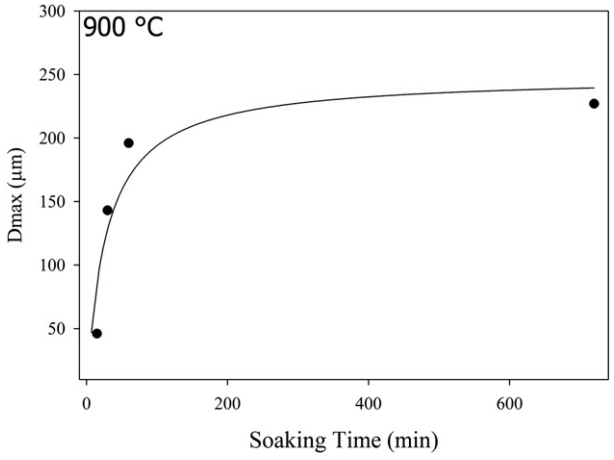

Fig. 9. The plot showing the dependence of the size of the maximum observed grain to the soaking time for the sample annealed at 900 °C.

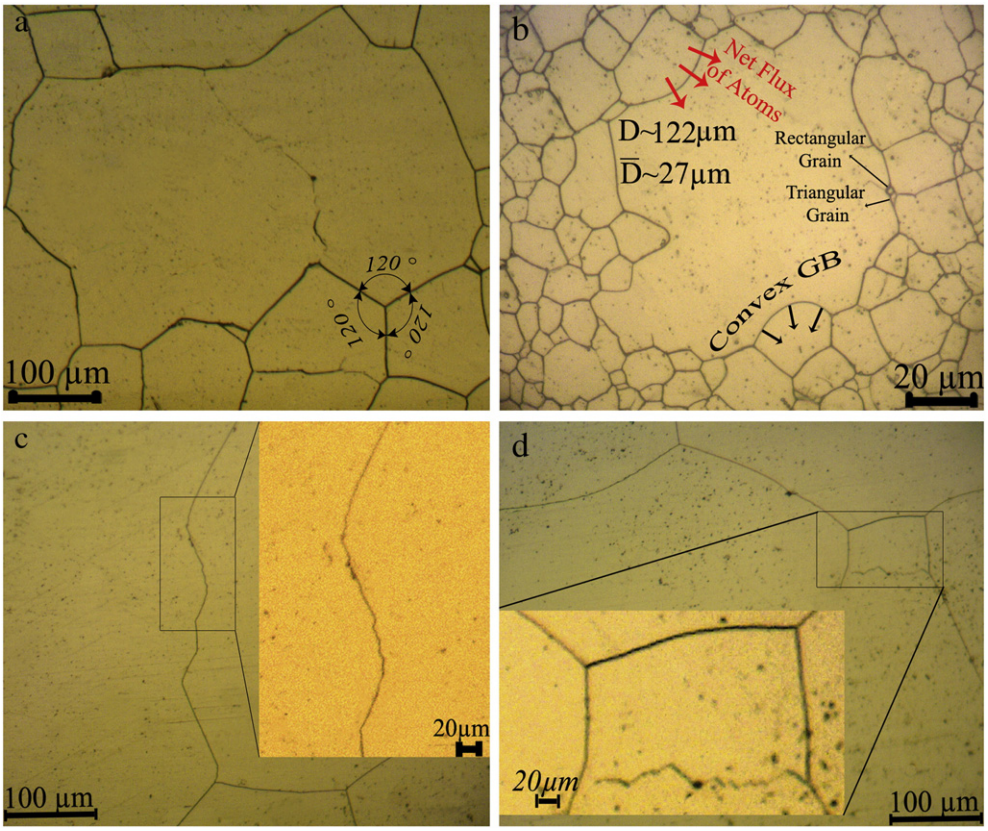

Fig. 10. The observed phenomena during abnormal grain growth: (a) sub-boundary enhanced solid-state wetting and also the evidence that the energy of the grain boundaries is isotropic, (b) annihilation of grains with less than 6 sides and the movement of concave grain boundaries toward their centers of curvature, and (c) and (d) probably grain boundary faceting.

lie on the triple junction line. Therefore, solid-state wetting along a triple junction can occur only when precipitates on triple junctions are dissolved. Near the dissolution temperature of precipitates, the precipitates on the triple junction dissolve faster than those on other locations such as grain boundaries and the bulk. In this situation, wetting along triple junctions occurs extensively whereas most grain boundaries are still pinned by precipitates which are not yet dissolved.

4. Conclusions

The following conclusions can be drawn from the study on the microstructural evolution during abnormal grain growth (secondary recrystallization) in 304L stainless steel in a wide range of annealing temperatures and times:

(1) At homologous temperatures lower than 0.65 (850 °C) and higher than 0.7 (900 °C) but lower than 0.8 (1100 °C), the grain growth mode was identified as normal for the annealing times considered in the current work.
(2) At homologous temperatures between 0.65 (850 °C) and 0.7 (900 °C), the observed transition in grain growth mode from normal to abnormal was detected to be caused by the dissolution/coarsening of carbides. This was demonstrated by the appearance of a bimodal grain size distribution histogram. However, continued annealing to a long time led to completion of secondary recrystallization and the subsequent reappearance of normal growth mode.
(3) In spite of the fact that the amount of titanium in the investigated alloy is significantly lower than the amount of vanadium, the XRD and EDAX analyses showed that the carbide particles are rich in Ti. Therefore, the matrix was found to be depleted of Ti. Vanadium was found to be present in both matrix and carbide particles.
(4) It was found that when the size of abnormal grains reached a certain value, their size will not change too much and the grain growth behavior becomes practically stagnant.
(5) Another instance of abnormal grain growth was observed at homologous temperatures higher than 0.8, which may be attributed to grain boundary faceting/defaceting phenomenon.

References

[1] F.J. Humphreys, M. Hatherly, Recrystallization and Related Annealing Phenomena, 2nd ed. Elsevier, UK, 2004.
[2] A.F. Padilha, R.L. Plaut, P.R. Rios, Annealing of cold-worked austenitic stainless steels, ISIJ Int. 43 (2003) 135–143.
[3] R.D. MacPherson, D.J. Srolovitz, The von Neumann relation generalized to coarsening of three-dimensional microstructures, Nature 446 (2007) 1053–1055.
[4] J.B. Koo, D.Y. Yoon, Abnormal grain growth in bulk Cu-the dependence on initial grain size and annealing temperature, Metall. Mater. Trans. A 32 (2001) 1911–1926.
[5] J.S. Choi, D.Y. Yoon, The temperature dependence of abnormal grain growth and grain boundary faceting in 316L stainless steel, ISIJ Int. 41 (2001) 478–483.
[6] Y.Z. Zhu, S.Z. Wang, B.L. Li, Z.M. Yin, Q. Wan, P. Liu, Grain growth and microstructure evolution based mechanical property predicted by a modified Hall–Petch equation in hot worked Ni76Cr19AlTiCo alloy, Mater. Des. 55 (2014) 456–462.
[7] Q. Sha, Z. Sun, Grain growth behavior of coarse-grained austenite in a Nb–V–Ti microalloyed steel, Mater. Sci. Eng. A 523 (2009) 77–84.
[8] Z. Huda, T. Zaharinie, Kinetics of grain growth in 2024-T3: an aerospace aluminum alloy, J. Alloys Compd. 478 (2009) 128–132.
[9] Y. XU, D. Tang, Y. Song, X. Pan, Prediction model for the austenite grain growth in a hot rolled dual phase steel, Mater. Des. 36 (2012) 275–278.
[10] S.J. Lee, Y.K. Lee, Prediction of austenite grain growth during austenitization of low alloy steels, Mater. Des. 29 (2008) 1840–1844.
[11] V.Y. Novikov, Microstructure evolution during grain growth in materials with disperse particles, Mater. Lett. 68 (2012) 413–415.
[12] P.R. Rios, M.E. Glicksman, Topological theory of abnormal grain growth, Acta Mater. 54 (2006) 5313–5321.
[13] J.C. Dutra, F. Siciliano, A.F. Padilha, Interaction between second-phase particle dissolution and abnormal grain growth in an austenitic stainless steel, Mater. Res. 5 (2002) 379–384.
[14] L.F. Li, J.P. Celis, Pickling of austenitic stainless steels (a review), Can. Metall. Q. 42 (2003) 365–376.

[15] H. Mirzadeh, A. Najafizadeh, ANN modeling of strain-induced martensite and its applications in metastable austenitic stainless steels, J. Alloys Compd. 476 (2009) 352–355.
[16] T. Maki, S. Shimooka, M. Umemoto, I. Tamura, The morphology of strain-induced martensite and thermally transformed martensite in Fe–Ni–C alloys, Trans. JIM 13 (1972) 400–407.
[17] H. Mirzadeh, A. Najafizadeh, Correlation between processing parameters and strain-induced martensitic transformation in cold worked AISI 301 stainless steel, Mater. Charact. 59 (2008) 1650–1654.
[18] H. Mirzadeh, A. Najafizadeh, Hot deformation and dynamic recrystallization of 17-4 PH stainless steel, ISIJ Int. 53 (2013) 680–689.
[19] G.F. Vander Voort, E.P. Manilova, J.R. Michael, A study of selective etching of carbides in steel, Microsc. Microanal. 10 (2004) 76–77.
[20] R. Abbaschian, L. Abbaschian, R.E. Reed-Hill, Physical Metallurgy Principles, 4th ed. Cengage Learning, USA, 2009.
[21] K.J. Ko, P.R. Cha, D. Srolovitz, N.M. Hwang, Abnormal grain growth induced by sub-boundary-enhanced solid-state wetting: analysis by phase-field model simulations, Acta Mater. 57 (2009) 838–845.